

spectrographic and 0.5 m Danish telescopes at La Silla. The 12.3 Å/mm coudé plates of  $\nu$  Cen were reduced at the ESO Data Reduction Centre in Garching, and the 3.3 Å/mm plates of  $\beta$  Cen were measured with the oscilloscope setting comparator at the Hoher List Observatory. Photoelectric observations were carried out with the aid of simultaneous four-channel uvby photometer. The results of these observations are shown in Fig. 2.

The radial velocity curves, in spite of their small amplitudes, are well defined and do not show any peculiarities. The accuracy of observations seems to be sufficient for determining both the moments of particular phases and the amplitudes (about 3 km/s for  $\nu$  Cen and 6 km/s for  $\beta$  Cen). Points denote velocities actually observed, the broken line is a sinusoid fitted by eye to the observations. Both objects are bright, so the exposure times were typically 2–3 min.

The high brightness of the stars complicates somewhat the photoelectric observations. Fortunately for  $\nu$  Cen a good comparison star exists, so the variability in the u-band with an amplitude of about 0.004 mag could be detected. The reality of the changes is confirmed by the observations made four nights later (open circles). Observations of  $\beta$  Cen were more difficult

and are certainly less accurate. This star (one of the brightest in the sky) could be observed only with appropriate shielding of telescope aperture. The only reasonable comparison is  $\alpha$  Cen differing largely in position and spectral type. Nonetheless, observations from two nights (dots and open circles), though not of excellent quality, strongly suggest the variability in the u-band with an amplitude of approximately 0.005 mag. (As was to be expected no trace of variability of these stars could be found in the B and V bands.)

Nevertheless, inspection of Fig. 2 immediately shows the different behaviour of the two stars. Phase relation between light and radial velocity in the case of  $\nu$  Cen obeys the general rule that in  $\beta$  Cephei stars the maximum of brightness occurs at the descending branch of the radial velocity. In this respect the behaviour of  $\beta$  Cen seems to be opposite: maximum of brightness—if real—corresponds clearly to the middle of the ascending branch.

It would be premature at the moment to draw any firm conclusion about the mode excited in  $\beta$  Cen from the direct comparison with Fig. 1. It seems clear, however, that observations of small amplitude  $\beta$  Cephei stars, although troublesome, are worth being done and may really contribute to our understanding of these objects.

## The Galactic Abundance Gradient

*P. A. Shaver and A. C. Danks, ESO*

*R. X. McGee and L. M. Newton, CSIRO Division of Radiophysics, Sydney*

*S. R. Pottasch, Kapteyn Astronomical Institute, Groningen*

### Introduction

The study of chemical abundances and their variation from one galaxy to another or within individual galaxies is of fundamental importance for our understanding of the evolution of galaxies. The abundances of heavy elements in the interstellar medium provide a fossil record of the enrichment which has taken place due to nucleosynthesis in successive generations of stars. Gradients of heavy element abundances with distance from the galactic centre are predicted by models in which the rate of star formation varies across the galactic disk, and by dynamical collapse models of galactic evolution which involve fresh infall of primordial gas onto the disk over long periods of time. Different models predict different abundance gradients (in slope and shape), and abundance measurements give constraints on these models (see Pagel and Edmunds, 1981, *Ann. Rev. Astron. Astrophys.* **19**, 77, for a recent review).

H II regions provide the most accessible probe of current interstellar abundances. In computing abundances from line intensity ratios, an accurate knowledge of the electron temperature is essential: a 40 per cent change in the temperature can change the abundance by an order of magnitude. Optically, temperatures can only be measured for the brightest and hottest H II regions, and this severely limits the number of H II regions for which "absolute" abundances can be determined.

Radio recombination lines can be used to obtain accurate electron temperatures for a much larger number of galactic H II regions. They are strongest when the temperature-sensitive optical lines are weakest, i.e. at low temperatures. In addition they can readily be detected from relatively faint or heavily reddened H II regions. Thus the radio and optical methods are truly complementary. By carefully choosing the radio recombination lines to be observed in accordance with the emission

measures of the H II regions, non-LTE corrections can be kept down to a few per cent, and uncertainties in the resulting temperatures are then limited only by observational factors, typically 5–10 per cent.

We have combined radio and optical spectroscopic observations of a large number of galactic H II regions in a novel approach to the determination of abundances and their distribution across the galactic disk. Accurate temperatures have been measured for 67 H II regions located between 3.5 and 13.7 kpc from the galactic centre; optical spectra have been obtained for 32 of these H II regions, bringing the total number of galactic H II regions with known (absolute) abundances from 18 to 43.

### Some Preliminary Results

The radio observations were made using the 210-foot radio telescope at Parkes in Australia. Sample spectra, showing the 109 $\alpha$  lines of hydrogen and helium, and the 137 $\beta$  line of hydrogen, are given in Fig. 1. These lines arise from transitions in the extreme outer parts of the atoms: the 109 $\alpha$  line is due to a  $n = 110 \rightarrow 109$  transition ( $n =$  principal quantum number), and the 137 $\beta$  line is due to a  $n = 139 \rightarrow 137$  transition. Of special interest in Fig. 1 is the narrowness of some of these lines, proving that some H II regions have electron temperatures below 5,000 K ( $\approx 15$  km s $^{-1}$ ).

Optical spectra were obtained using the Image Dissector Scanner (IDS) and the Image Photon Counting System (IPCS) on the ESO 3.6-m telescope, and with the IPCS at the Anglo-Australian Telescope. Fig. 2 shows a representative selection of these spectra. Variations in excitation conditions, temperature, and abundances are revealed by changes in the [O III]/H $\beta$

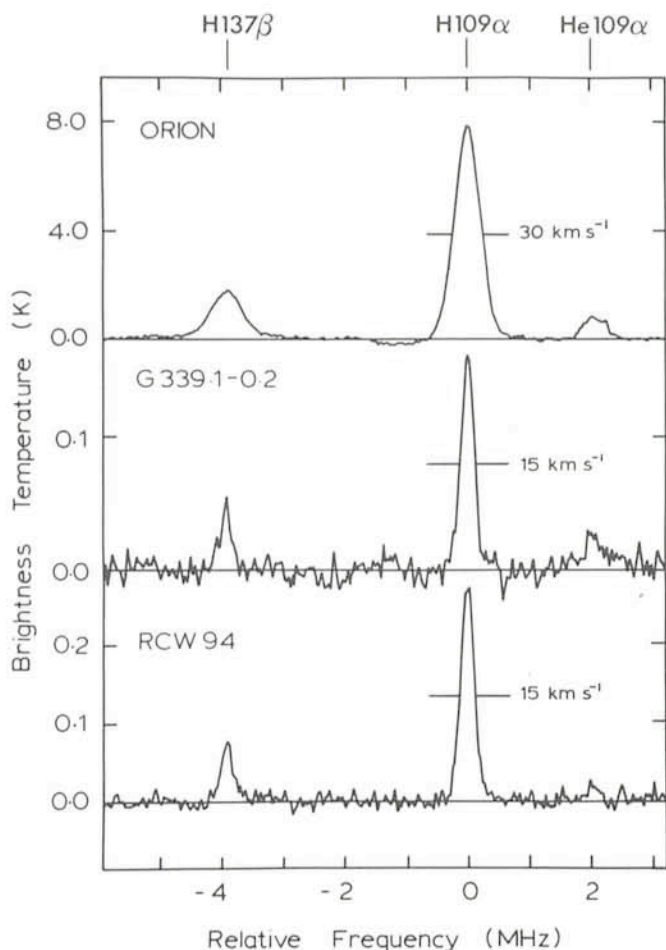


Fig. 1: Radio spectra of three galactic H II regions at 5 GHz, showing recombination lines of hydrogen and helium. Note particularly the narrowness of the lines from G 339.1-0.2 and RCW 94, proof that their electron temperatures are less than 5,000 K.

and [N II]/H $\alpha$  ratios. The strong reddening evident in the bottom three spectra highlights the difficulty in finding candidates for optical observations in the important region within 7 kpc of the galactic centre.

The radio-determined electron temperatures, corrected for the small deviations from LTE, were applied to these optical spectra to compute abundances. At this point an additional uncertainty enters, related to possible stratification effects within each H II region: the temperatures of the O $^+$ , O $^{++}$ , N $^+$ , and H $^+$  zones may differ significantly from each other. Photoionization models (such as those by Stasinska, 1980, *Astron. Astrophys.* **84**, 320) suggest that such differences can be important especially below 7,000-8,000 K. Thus the derivation of abundances from optical spectra using radio temperatures is to some extent model-dependent, and the uncertainty is greatest at low temperatures (and therefore in the inner regions of the galaxy).

Fig. 3 shows the electron temperatures (from the radio data), the He $^+$ /H $^+$  ratios (from radio and optical data), and preliminary oxygen and nitrogen abundances (from the radio temperatures, the optical spectra, and one set of models), plotted against galactocentric distance. Gradients are clearly present in  $T_e$ , O/H, and N/H, but not in He $^+$ /H $^+$ .

The  $T_e$  and O/H gradients are mutually consistent, on the assumption that oxygen is the prime coolant in H II regions. On the other hand, the range of temperatures at a fixed  $R_G$  is due in large part to the range of effective temperatures of the exciting

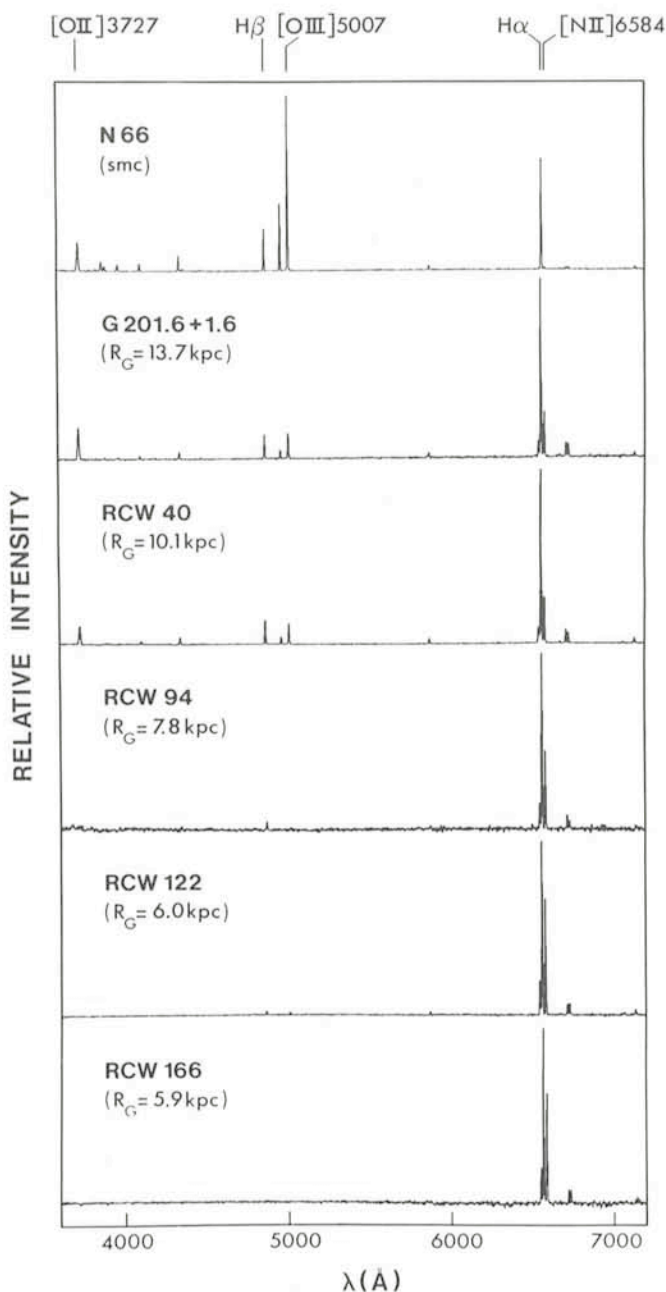


Fig. 2: Optical spectra of six representative H II regions, showing the wide range of excitation and reddening found in the sample.

stars and to the range of densities of the H II regions: most of this spread is real, and not due to observational error.

The absence of any significant gradient in He $^+$ /H $^+$  may be due to two effects which roughly balance each other. The total helium abundance may increase with metallicity, i.e. towards the galactic centre, due to helium production in stars. On the other hand the increasing metallicity may reduce the relative number of helium-ionizing photons, and therefore the He $^+$ /H $^+$  ratio, due to line blanketing in the stellar atmospheres.

Finally, the similarity of the oxygen and nitrogen abundance gradients is surprising, because these are thought to be primary and secondary nucleosynthesis products respectively. Primary elements have  $^1\text{H}$  or  $^4\text{He}$  as their direct progenitors, whereas secondary species are formed by subsequent processing of a primary element. Thus, the abundance of a secondary element should increase as the square of the abundance of its primary progenitor. Most metals do vary in

lockstep with oxygen, as expected for primary elements. The fact that the nitrogen abundance gradient is not much steeper suggests that much of the nitrogen may also be of primary origin. A further puzzle arises in the fact that several isotopic ratios ( $^{18}\text{O}/^{17}\text{O}$ ,  $\text{C}/^{13}\text{C}$ ,  $\text{S}/^{34}\text{S}$ ,  $\text{N}/^{15}\text{N}$ , etc.), measured at millimeter wavelengths, are constant to a high degree over the plane of

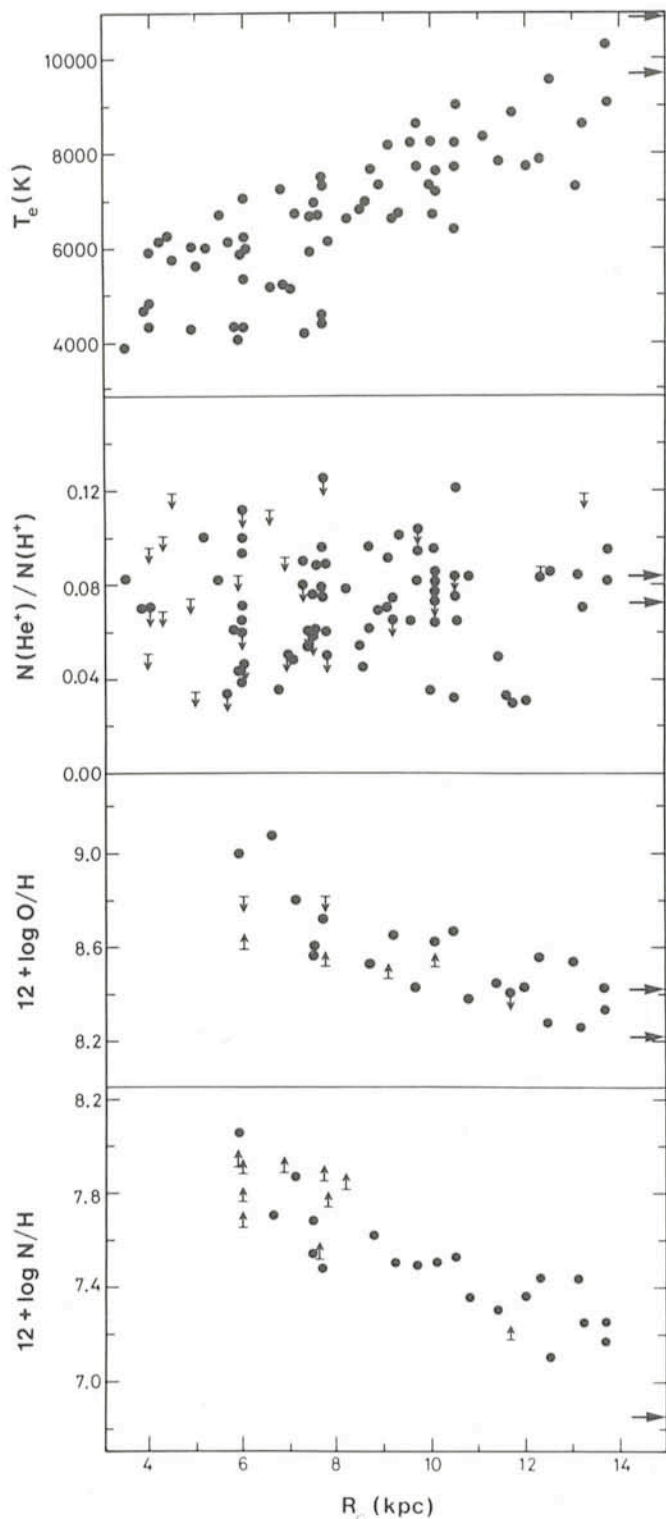


Fig. 3: Variations of electron temperature and preliminary abundance ratios  $\text{He}^+/\text{H}^+$ ,  $\text{O}/\text{H}$ , and  $\text{N}/\text{H}$ , as a function of distance from the galactic centre. Arrows to the right indicate values for the LMC (30 Doradus) and SMC (N66).

the galaxy, in apparent contradiction to the marked gradients in  $\text{O}/\text{H}$ ,  $\text{S}/\text{H}$ , etc. (Wannier, 1980, *Ann. Rev. Astron. Astrophys.* **18**, 399). These facts seem to call for a revision of our ideas about nucleosynthesis.

It is thought that the disk of our galaxy formed gradually, with infall of primordial gas extending over a long period. The main evidence for this is the shortage of old stars in the disk with low abundances. These infall models share the prediction that the abundance gradient should flatten off in the inner regions of the disk (Tinsley and Larson, 1978, *Astrophys. J.* **221**, 554; Chiosi, 1980, *Astron. Astrophys.* **83**, 206). There is no evidence for this in Fig. 3, but there are a number of ways out of this dilemma, such as postulating infall of metal-enriched gas from stars in the galactic bulge. There are clearly many free parameters in such models, but an increasing array of observational data will hopefully provide the constraints necessary to ultimately distinguish the actual evolutionary scenario.

## List of Preprints Published at ESO Scientific Group

December 1981 – February 1982

177. J. Breysacher, A.F.J. Moffat and V.S. Niemela: Wolf-Rayet Stars in the Magellanic Clouds. II. The Peculiar Eclipsing Binary HD 5980 in the SMC. *Astrophysical Journal*. December 1981.
178. E. Athanassoula, A. Bosma, M. Crézé and M.P. Schwarz: On the Sizes of Rings and Lenses in Disk Galaxies. *Astronomy and Astrophysics*. December 1981.
179. I.S. Glass, A.F.M. Moorwood and W. Eichendorf: Mid-Infrared Observations of Seyfert 1 and Narrow-Line X-ray Galaxies. *Astronomy and Astrophysics*. December 1981.
180. S. D'Odorico and M. Rosa: Wolf-Rayet Stars Associated to Giant Regions of Star Formation. IAU Symposium 99 on Wolf-Rayet Stars. December 1981.
181. J. Materne, G. Chincarini, M. Tarenghi and U. Hopp: Optical Investigations of Two X-ray Clusters of Galaxies: 0430.6-6133 and 0626.7-5426. *Astronomy and Astrophysics*. January 1982.
182. M. Rosa and S. D'Odorico: Wolf-Rayet Stars in Extragalactic H II Regions: II. NGC 604—A Giant H II Region Dominated by many Wolf-Rayet Stars. *Astronomy and Astrophysics*. January 1982.
183. W. Bijleveld and E.A. Valentijn: Radio and X-ray Observations of the Abell 2241 Galaxy Clusters. *Astronomy and Astrophysics*. January 1982.
184. Ch. Motch, J. van Paradijs, H. Pedersen, S.A. Ilovaisky und C. Chevalier: Visual and Infrared Photometry of 2A 0311-227. *Astronomy and Astrophysics*. January 1982.
185. L. Woltjer and G. Setti: Quasars in the Universe. To be published in the Proceedings of the Vatican Study Week on "Cosmology and Fundamental Physics", Rome, Sept. 28–Oct. 2, 1981. February 1982.
186. G. Setti and L. Woltjer: The Origin of the X- and  $\gamma$ -ray Backgrounds. To be published in the Proceedings of the Vatican Study Week on "Cosmology and Fundamental Physics", Rome, Sept. 28–Oct. 2, 1981. February 1982.
187. R. Barbon, M. Capaccioli, R.M. West and R. Barbier: Redshifts of Parent Galaxies of Supernovae. *Astronomy and Astrophysics*, Suppl. February 1982.
188. R.M. West and H.E. Schuster: The ESO Quick Blue Survey and ESO (B) Atlas. *Astronomy and Astrophysics*, Suppl. February 1982.
189. W. Eichendorf, A. Heck, B. Caccin, G. Russo and C. Sollazzo: UV, Optical and IR Observations of the Cepheid R. Muscae. *Astronomy and Astrophysics*. February 1982.
190. M.P. Véron-Cetty, P. Véron and M. Tarenghi: Are All Galactic Nuclear Regions Sodium Rich? *Astronomy and Astrophysics*. Februar 1982.